Sulforaphane Enhances the Anticancer Properties of Paclitaxel in Two Human Derived Prostate Cancer Cell Lines

Tito N. Habib (titohabib99@science.sohag.edu.eg)
Sohag University
Mohamed O. Altonsy
Sohag University
Salah A. Ghanem
Sohag University
Mohammed S. Salama
Ain Shams University
Mai A. Hosny
Sohag University

Research Article

Keywords: Sulforaphane, Paclitaxel, Drug resistance, Prostate Cancer, Flow Cytometry, Cell Cycle, Synergistic

Posted Date: April 15th, 2022

DOI: https://doi.org/10.21203/rs.3.rs-1552332/v1

Abstract

Background

In cancer therapy, combined treatment results in synergistic or additive outcomes and reduces the development of drug resistance in response to anticancer agents compared with monotherapy. We propose that when Paclitaxel (Taxol, PTX) is combined with sulforaphane (SFN), may result in better treatment outcomes in prostate cancer.

Methods

We measured apoptosis, cell cycle, and expression of Bax and Bcl_2 in response to the PTX and SFN individual and combined treatments. Cell lines (PC-3) and (LNCaP), were individually treated with different concentrations of PTX, SFN, and its combination. Annexin V/PI positivity and data analysis were conducted using a flow cytometer and guava data acquisition and analysis software. Graph-Pad Prism 6, and Microsoft Excel software were used for statistical analyses and graphs generation. Student's t-tests or one-way analysis of variance with Tukey's correction were used to determine the significant difference between treatments.

Results

The effect of the PTX or SNF treatments on reducing cell viability increased in a dose-dependent manner. Combined treatment enhanced PTX's effects and reduced the EC_{50} values of both drugs compared to individual treatments. Flow cytometry analysis revealed that PTX or SFN treatments redistributed cell-cycle phases by inducing S-phase arrest and increasing apoptotic cell population in PC-3 cells. Such effects were enhanced in the PTX + SFN combination group. Interestingly, the necrotic cells' numbers were not affected by the combination treatments. Caspase-3 cleavage and morphological deformations of the cell nuclei are signs of apoptotic cell death; such parameters were examined by western blot and fluorescent microscopy in response to individual and combination treatments.

Conclusion

The PTX or SNF differentially modulated the expression of Bax and Bcl_2 in PC-3 and LNCaP cell lines, and the combined treatment enhanced these effects in favor of cell apoptosis versus survival. These findings will help develop new biomarkers and guide therapy choices.

Background

Combination therapy is a recommended intervention in which the patient receives more than one therapy. Treatment regimens involving the administration of several separate pills, each containing a specific drug, or single pills containing different drugs are examples of combination therapy.

In men, prostate cancer is the sixth leading cause of death. Worldwide disease statistics revealed that over one million men were diagnosed with prostate cancer, and the number of deaths exceeded three hundred thousand in the year 2012 only. These numbers ranked prostates cancer the second among commonly diagnosed cancers in

men [1]. The prostate gland secretes alkaline fluid in the male's reproductive system as part of semen, which functions as a pH buffer to protect the sperms [2]. Enlargement of the prostate gland is a common age-related symptom known as benign prostatic hypertrophy (BPH). However, BDH is noncancerous; it may result in unpleasant clinical symptoms, such as urination problems, infections, and even kidney diseases [3]. The development of prostate cancer is gradual and occurs over a prolonged period, which makes the early diagnosis utterly challenging. However, the etiology of the disease is widely heterogeneous; myriad studies have highlighted genetics, ageing, obesity, and ethnicity as major risk factors [4]. Recently, researchers have studied the role of dietary habits in the incidence of prostate cancer and pointed at high intakes of dairy products, red meats, processed meats, foods rich in α-linolenic acid, and calcium as possible risk factors [5–7]. Such research has created a groundswell of eagerness to study the influences of certain dietary components on human health/disease status.

The SFN (1-isothiocyanato-4-methyl-sulfinyl butane), a compound naturally found in cruciferous vegetables, has potential therapeutic properties, such as detoxification, antimicrobial, anti-inflammatory, and redox balancing [8]. SFN's therapeutic and protective properties may attribute to the induction of the nuclear factor-erythroid-2-related factor 2 (Nrf2) transcription factor, which regulates antioxidant response elements, inflammation, non-enzyme antioxidants, and phase II detoxification enzymes [9]. Interestingly, the anti-cancerous properties of SFN were reported before the identification of the Nrf2 gene [10]; when Zhang *et al.* [11] and Prochaska *et al.* [12] confirmed that SFN induced the expression of quinone reductase and glutathione transferases (phase II anticarcinogenic enzyme) in murine hepatoma cells. Furthermore, SFN induces other cytoprotective enzymes, for example, NAD(P)H: quinone reductase-1 (Nqo1), haemoxygenase-1, glutamate-cysteine ligase, glutathione peroxidase, thioredoxin, thioredoxin reductase, and Peroxisome proliferator-activated-γ (PPAR-γ) [13, 14]. Due to its promising therapeutic properties, SFN has been focused on by researchers and utilized to treat different types of cancers [15].

The role of SFN in human prostate cancer was previously studied by Brooks *et al*. [16] and Singh *et al*. [17]. They reported potent induction of phase II enzymes and initiation of reactive oxygen species following SFN treatment. SFN also showed a protective effect against prostate cancer recurrence and significantly lowered the prostate-specific antigen (PSA) progression after radical prostatectomy [18]. Additionally, Beaver *et al*. [19] stated that SFN decreased upregulated histone deacetylase (**HDAC3**) protein expression in transgenic adenocarcinoma of the mouse prostate.

In cancer treatment, combined therapy results in synergistic or additive outcomes, and reduces the development of drug resistance in response to anti-cancer agents compared with monotherapy [20]. The PTX is an anti-cancer drug that targets actively dividing cells by halting their mitosis, arresting cell growth, and ultimately initiating apoptotic cell death [21]. Here, we compared the outcomes of combined and monotherapies of SFN and PTX in prostate cancer cell lines (PC-3 and LNCaP). We applied molecular biology techniques to measure apoptosis, cell cycle arrest, and the expression of **Bax** and **Bcl2** proteins in response to the two different treatment strategies.

Materials And Methods

Cell lines and reagents

Prostate cancer adenocarcinoma cell line PC-3 (catalog no. CRL-1435; ATCC), and prostate carcinoma cell line LNCaP (catalog no. CRL-1740; ATCC), were cultured in RPMI-1640 (catalog no. 12633-012; Gibco) complete growth medium sublimated with 10% heat-inactivated fetal bovine serum (FBS) (catalog no. 098105; Multicell). Seeded

cells were incubated at 37°C and 5% CO_2 atmosphere; the medium was changed every 48 h. 80% confluent cells were then dissociated using 0.25% trypsin (catalog no. 15400-054; Gibco) and plated in 24-well cell culture plates at a density of 70,000 cells/well for 24 h before treatment. PTX (catalog no. T7402; Millipore Sigma) was dissolved in dimethyl sulfoxide (DMSO, catalog no. d5879; Sigma-Aldrich) at a concentration of 50 mg/mL. Sulforaphane (SFN) (catalog no. s4441; Millipore-Sigma) was diluted in DMSO to a concentration of 5mg/mL. Different concentrations of PTX or SFN were freshly prepared in a complete culture medium before treatment.

Cell viability assay:

For cell viability assay we used Thiazolyl blue tetrazolium bromide (MTT) (catalog no. m-5655; Sigma). Briefly, we dissolved MTT in phosphate-buffered saline at a concentration of 5 mg/mL. after treating the cells with PTX, SFN, or PTX + SFN, we added MTT to each well of 24-well plates at a final concentration of 1 mg/mL directly to the culture medium. Plates were then incubated at 37°C for three hours, and then we removed the culturing medium and dissolved MTT formazan crystals in 500 µL MTT solvent (4 mM HCL, catalog no. acs393; BDH, 0.1% Nonidet P40, catalog no. 74385; Fluka, in isopropyl alcohol, catalog no. un1219; Omnisolv) on a rocker in dark for 15 minutes. 100 µL of the dissolved MTT crystals were transferred to each well in a 96-well plate and were read on a SPECTRAmax PLUS384 Microplate spectrophotometer set to 590 nm wavelength.

Cell lysate preparation, total protein quantification, and Western blot analysis:

Following the treatments, the culture medium was removed, and cells were harvested in Radioimmunoprecipitation assay buffer (RIPA) containing a 1 × protease inhibitor cocktail (catalog no. PI-78439c; Thermo Scientific). Total protein quantification was conducted using BioRad protein assay (catalog no. 500-0006; BioRad) following the manufacturer's protocol. Total protein was denatured by adding 2× Laemmli buffer (SDS, 4%; β-mercaptoethanol, 10%; glycerol, 20%; bromophenol blue, 0.004%; Tris-HCl, 0.125 M), 1:1 (v/v) and boiled at 95°C for 5 min. Then protein (50 µg/sample) was loaded into 10% SDS-polyacrylamide gel electrophoreses. BLUelf pre-stained protein ladder (catalog no. PM008-0500; Frogga Bio) was used as a molecular weight marker (5-245 KDa). Separated protein bands were transferred to a nitrocellulose membrane (catalog no. rpn203D; EG Healthcare). Membranes were immune-probed with rabbit polyclonal anti caspase-3 (catalog no. AAP-113E; Stressgen), rabbit A monoclonal anti-Bax (catalog no. ab32503; Abcam), rabbit monoclonal anti-Bcl_2 (catalog no. ab32124; Abcam) and anti-glyceraldehyde-3-phosphate dehydrogenase (anti-GAPDH) (catalog no. 4699–9555; Biogenesis). To detect the immune-probed protein bands we used the secondary antibodies peroxidase-affiniPure goat anti-mouse IgG (catalog no. 115-035-003; Jackson ImmunoResearch) or peroxidase-conjugated goat anti-rabbit IgG (catalog no. 111-035-003). Band visualization and densitometric analysis were carried out using Pierce ECL Western Blotting Substrate (catalog no. PI-32106; Thermo Fisher Scientific), Chemi Doc XRS system, and image Lab 6.0 software (BioRad).

Fluorescent microscopy and image analysis

We grew the cells (70,000 cells/well) on coverslips placed at the bottom of each well in 24-well plates for 24 h before treatment. Cells were then fixed in ice-cold methanol (catalog no. a412; fisher chemicals) for 10 minutes at -20°C. Methanol treatment permeabilized the cell membrane and allowed 4',6-diamidino-2-phenylindole (DAPI, catalog no. d21490; Molecular Probes) to penetrate and stain the nuclear chromatin. DAPI was prepared in PBS at a concentration of 300 nM and added to the cell monolayers for 5 minutes followed by three washes (5 minutes

each) in PBS. Cells were mounted using prolonged gold anti-fade reagent (catalog no. p36930; Invitrogen) and visualized with confocal microscopy (Zeiss, Oberkochen, Germany) using ZEN 2012 software.

Propidium iodide (PI) staining and cell cycle analysis

After treatment, PC-3 cells were fixed for 30 minutes in 70% ethanol at 4°C. Cells were washed twice in PBS, and 100 µg/ml of RNase A (catalog no. 1007885; Qiagen) was added, and the cells were incubated for 20 minutes at 37°C, followed by two washes with PBS. Cells were then incubated in 3 µM PI (catalog no. P4170; Sigma) in the staining buffer (100 mM tris, pH 7.4, 150 mM NaCl, 1 mM $CaCl_2$, 0.5 mM $MgCl_2$, 0.1% Nonidet P40) for 15 minutes at room temperature. Cell cycle analysis was carried out using a Flow cytometer (Guava® easy Cyte; Millipore Sigma). Data analysis was carried out using guava cell cycle data acquisition and analysis software (Guava Technologies).

Annexin V and PI Dual staining and Flow cytometry analysis:

Harvested PC-3 cells were washed twice in PBS and resuspended in annexin V binding buffer (10 mM Hepes (pH 7.4), 140 mM NaCl, and 0.25 mM $CaCl_2$). Add annexin V-FITC conjugated (catalog no. A13199; Thermo-Fisher) at a concentration of 1:100 and incubate the cells in the dark for 15 minutes at room temperature. PI was added at a final concentration of 3 µM and cells were incubated in the dark for 15 minutes at room temperature. Stained cells were washed twice in annexin V binding buffer and fixed in 1% formaldehyde prepared in annexin V binding buffer for 10 minutes on ice. Cells were then washed twice in PBS and RNase A was added at a final concentration of 100 µg/ml and cells were incubated for 20 minutes at 37°C. Cells were washed twice and resuspended in PBS. Annexin V/PI positivity and data analysis were conducted using a flow cytometer (Guava® easyCyte; MilliporeSigma) and guava data acquisition and analysis software (Guava Technologies).

Statistical analysis.

Data were obtained from *n* independent biological experiments and are depicted as plots of the mean of individual values with SD error bars, or box-and-whisker plots showing the median, the 25th, and 75th quartiles, as well as the minimum to maximum values. Western blot densitometric analysis was carried out using the ChemiDoc XRS system and image Lab 6.0 (BioRad) and TotalLab TL120. Graph-Pad Prism 6, and Microsoft Excel software were used for statistical analyses and graphs generation. Student's t-test (for two groups comparison) or one-way analysis of variance (ANOVA) with Tukey's correction (for multiple comparisons) were used to determine the significant difference between PTX, SFN, PTX + SFN, and the PC-3 non-stimulated cells (NS), which had not received any therapies.

Results

Cell viability dose-response analysis to evaluate the effect of SFN on antiproliferation effects of PTX in PC-3 cells:

PC-3 cells were grown in a complete medium in 48-well plates, at a cell density equal to 35,000 cells per well, for 24 h. Different concentrations of PTX or SFN were prepared as indicated in the method section and used to treat the cells. MTT assay was conducted 24 h post-treatment, and the percentage of cell viability was determined for each drug concentration. Our data revealed that PTX and SFN significantly reduced PC-3 cell viability in a dose-dependent manner (Fig. 1). Meanwhile, the EC_{50} was higher in PTX (1.2 mg/ml) than in SFN-treated cells (18.7 µg/ml).

The SFN synergized PTX effect on reducing PC-3 cell viability:

To determine the effect of PTX in combination with SFN on the cell viability of PC-3 cells, we dissolved both drugs at equal concentrations starting at 100 ng/ml to 2500 µg/ml. Our results demonstrated that combined treatment synergized the effects of both drugs on reducing cell viability. EC_{50} of the combination was 3.5 µg/ml, which was 342 and 5.3-fold lower than PTX and SFN individual treatments, respectively (Fig. 2 A). We compared the percentages of viable cells following the treatment with PTX or SFN individually and the combination in a separate experiment. Our results showed that the PTX in combination with SFN had a significantly more potent effect on reducing PC-3 cell viability, even at a concentration as low as 2 µg/ml, where PTX+SFN significantly reduced cell viability to 70.86% ($p \leq 0.013$) compared to cell viability values of the PC-3 non-stimulated cells, which were considered as 100%. At the same concentration of 2 µg/ml, neither PTX nor SFN individual treatments showed significant effects on reducing the percentage of viable PC-3 cells ($p \geq 0.05$) (Fig. 2B). The effect of the combination treatment continued incrementally by increasing the drugs' concentration up to 8 µg/ml, and higher concentrations did not improve such effects on reducing cell viability.

The combination of PTX and SFN augmented PTX-induced Caspase-3 activation and nuclear morphology changes characterize apoptotic cell death in PC-3 cells:

Caspase 3 activation and changes in cell nuclei morphology, such as nuclear fragmentation and micronuclei appearance, are hallmarks for apoptotic cell death. To evaluate the effect of PTX and/or SFN treatments on inducing apoptosis in PC-3 cells, we treated the cells as described in the methods section. We utilized western blot analysis and fluorescent microscopy to detect caspase 3 activation, and the nuclei morphological changes. As expected, PTX or SFN treatment resulted in the cleavage of pro-caspase 3 protein into smaller active caspase 3 subunits, which was detected by western blot at ~17kDa. Densitometric analysis of caspase 3 protein bands revealed that the intensity of cleaved caspase 3 bands in the protein lysate of PC-3 cells treated with the combination was significantly higher than in the protein lysates of cells treated with PTX or SFN individually (Fig. 3A).

Microscopic visualization of DAPI stained nuclei depicted morphological changes, such as chromatin condensation, micronuclei, nuclear fragmentation, and a noticeable reduction in the number of nuclei in the visualized fields may be due to the detachment of cells after treatments. Such effects were not observed in the PC-3 non-stimulated cells, where the normal round nuclei appearance prevailed (Fig. 3B). Moreover, the described apoptotic cell death characteristics were more prominent in the cells that received PTX+SFN combined treatment when compared with any single agent alone. These results suggest that SFN in combination with PTX can increase the effectiveness of PTX in triggering apoptosis in PC-3 cells.

The effect of the PTX and SFN Combination on redistributing the cell-cycle growth phases in PC-3 cells was more prominent than it was in individual treatments

To study the effect of PTX and/or SFN on cell cycle growth phases in the PC-3 cells, we stained the cells with propidium iodide and ran the cells on the Flow cytometer as described in the methods section. PTX or SFN treatments increased the percentage of the sub-G_1 population by 9.23-fold ($p \leq 0.0002$) or 9.10-fold ($p \leq 0.0006$), respectively, compared to non-stimulated cells. The effect of combined treatment was statistically more significant than PTX or SFN individual treatments and increased the sub-G1 population by 14.98-fold ($p \leq 0.0001$) compared

to the PC-3 non-stimulated cells. Such an increase was 1.6-fold ($p \leq 0.003$) and 1.7-fold ($p \leq 0.002$) higher than PTX or SFN individual treatments, respectively (Fig. 4A). Initially, an increasing sub-G_1 population is indicative of the occurrence of apoptotic cell death, and our data confirmed that such an effect was augmented when cells received the PTX+SFN combined treatment. Furthermore, PTX or SFN induced an S-phase growth arrest by 6.38% ($p \leq 0.01$) or 3.1% ($p \leq 0.05$), respectively. Again, combination treatment enhanced this effect to reach 9.93% ($p \leq 0.002$). To study the necrotic effects of the PTX and/or SFN, we double-stained the PC-3 cells with PI and annexin V and counted the necrotic cells using the Flow cytometer. Our results demonstrated that PTX or SFN treatments increased the number of necrotic cells to 5.23-fold ($p \leq 0.0002$) or 5.74-fold ($p \leq 0.0003$), respectively, compared with non-stimulated cells. Interestingly, there was no significant difference among the fold-change values of necrotic cells in PTX, SFN, and the combinations ($p \geq 0.05$); where the combined treatment increased the number of necrotic cells to 5.71-fold ($p \leq 0.0002$) compared to necrotic cell numbers in the PC-3 non-stimulated cells, which is similar to those fold change values of the PC-3 cells individually treated with PTX or SFN (Fig. 4B).

The PTX and SFN combination had a stronger effect on modulating Bax and Bcl_2 protein expression than the PTX or SFN individual treatment in PC-3 and LNCaP cells:

Protein lysates prepared from the PC-3 cell line were separated on SDS-PAGE and the protein bands were transblotted to nitrocellulose membranes and immune-probed against Bax, Bcl_2, and GAPDH. Bands' visualization and densitometric analysis revealed significant increases in Bax protein expression by 185.08% ($p \leq 0.04$) or 224.56% ($p \leq 0.01$) following PTX or SFN treatments, respectively. We observed an additive effect on increasing Bax protein levels when cells were subjected to the combined treatment by 353.56% ($p \leq 0.0002$), all numbers and statistical significance calculations are depicted in Tables 1&2. Bcl_2 showed opposite expression patterns to Bax, where PTX or SFN reduced Bcl_2 expression in PC-3 cells. The additive effect on reducing Bcl_2 levels was also observed after the combined treatments (Tables 1&2).

For further investigation, we calculated the ratio between Bax and Bcl_2 protein expression; we found a significant increase in such ratios in PC-3 cells treated with PTX or SFN compared to the PC-3 non-stimulated cells by 3.54-fold ($p \leq 0.0007$) or 3.4-fold ($p \leq 0.002$), respectively. PTX+SFN combined treatment increased Bax/Bcl_2 ratio to 9.68-fold ($p \leq 0.0006$) (Table 1 & Fig. 5A). To confirm our findings, we utilized another prostate cancer cell line, LNCaP, and again we treated the cells with PTX, SFN, or with the combination of PTX+SFN as described in the methods section. The data we collected from LNCaP cells confirmed that the PTX or SFN increases the protein expression of Bax and reduces Bcl_2 levels, thus increasing the ratio of Bax/Bcl_2. Such effects were augmented with the combined treatment of PTX+SFN (Table 2 & Fig. 5B).

Table 1. Bax and Bcl_2 protein expression in response to PTX, SFN, or PTX+SFN in PC-3 prostate can line. The numbers below are densitometric arbitrary scan units of the protein bands norma GAPDH, and the statistical analysis we performed to calculate the percentages of change in expression in treated cells compared to non-stimulated control cells (NS), and among the d treatments. Data $n = 5$, $*p \leq 0.05$, $**p \leq 0.01$, $***p \leq 0.001$.

Treatment	Proteins	Replicates					Mean	% Change relative to control (NS)
		1	2	3	4	5		
Control (NS)	Bax	18.219	15.741	12.053	22.415	8.834	**15.452**	--
	Bcl_2	20.183	19.178	17.072	26.614	9.700	**18.549**	--
PTX	Bax	27.247	36.896	37.402	22.455	19.00	**28.600**	185.5, $(p \leq 0.04)^{*}$
	Bcl_2	10.150	10.852	10.839	7.856	7.820	**9.503**	-48.7, $(p \leq 0.03)^{*}$
SFN	Bax	29.262	45.506	33.076	26.875	38.788	**34.701**	225, $(p \leq 0.01)^{**}$
	Bcl_2	10.541	12.272	13.083	13.049	11.548	**12.099**	-34.7, $(p \leq 0.06)^{ns}$
PTX+SFN	Bax	58.276	52.356	49.687	73.253	39.698	**54.654**	353.6, $(p \leq 0.0002)^{***}$
	Bcl_2	6.5010	9.905	5.455	7.860	5.056	**6.956**	-62.5, $(p \leq 0.007)^{**}$

Table 2. Bax and Bcl2 protein expression in LNCaP prostate cancer cell line in response to PTX, PTX+SFN treatments. The numbers below represent densitometric arbitrary scan units of the bands adjusted to GAPDH, and the statistical analysis we used to measure the percentages of cl protein level in treated cell groups compared to non-stimulated control cells (NS), including the treatments. Data $n = 5$, $^{*}p \leq 0.05$, $^{**}p \leq 0.01$, $^{***}p \leq 0.001$.

Treatment	Proteins	Replicates					Mean	% Change relative to control (NS)
		1	2	3	4	5		
Control (NS)	Bax	23.887	24.286	24.642	17.588	26.354	**23.351**	--
	Bcl_2	54.386	62.535	49.696	79.053	53.199	**59.774**	--
PTX	Bax	41.620	40.590	42.333	49.349	28.784	**40.535**	173.5, $(p \leq 0.02)^{*}$
	Bcl_2	36.924	46.211	25.262	52.320	26.762	**37.496**	-37.2, $(p \leq 0.0005)^{***}$
SFN	Bax	49.388	44.033	65.5122	43.501	60.101	**52.507**	224.8, $(p \leq 0.003)^{**}$
	Bcl_2	32.839	33.793	41.586	37.678	32.274	**35.634**	-40.3, $(p \leq 0.01)^{**}$
PTX+SFN	Bax	50.525	41.535	82.354	58.673	49.436	**56.505**	241.9, $(p \leq 0.01)^{**}$
	Bcl_2	10.270	6.166	12.411	9.840	12.438	**10.225**	-82.8, $(p \leq 0.001)^{***}$

Discussion

In the United States, there are approximately 10,000 ongoing clinical trials investigating combination therapies for cancer, infectious diseases, metabolic, cardiovascular, autoimmune, and neurological disorders. Combination therapies are compared to single drugs and are considered effective if they produce a better response when administered together than if they are taken individually. However, because many drug combinations could have additive or even synergistic effects, the degree of synergy becomes the most important factor to consider. To answer it, the two-drug combination should be compared to not only single treatments but also the best of previously reported drug combinations [22].

PTX has been used as an anticancer agent for treating a variety of cancers since 1989; its therapeutic outcomes did not meet the high expectations of physicians, rather than patients; because many types of cancers, such as prostate, breast, ovarian cancers resist PTX treatment [23, 24]. In our endeavors to improve the anticancer potency of PTX, we proposed that combining PTX and SFN, another promising and naturally existing phytochemical found primarily on green cruciferous vegetables, may result in better treatment outcomes in prostate cancer cell models. Since 1987, when Levin and Hryniuk [25] introduced the concept of drug dose-intensity, the dose, and duration of a

given drug are precisely calculated to deliver the maximum tolerated dose to overcome resistance to such chemotherapeutic agents. High drug doses are most likely accompanied by severe side effects, which is why researchers aspire to any therapeutic regimens that would lead to lowering the dose and consequently the side effects and maintaining the efficacy of the drug. The data presented here showed that combining PTX and SFN dramatically lowered the EC_{50} of both drugs compared to the EC_{50} values of the same drugs when administrated individually. If applied to prostate cancer patients, such findings may benefit them and help avoid or attenuate the side effects of high doses.

Apoptosis is a natural process through which the body eliminates unwanted and damaged cells. A balanced apoptosis/cell division rate protects from the occurrence of uncontrolled cell division and ultimately the development of cancers [26]. Unlike necrosis, apoptotic cell death does not elicit an inflammatory response and allows the body to recycle the dead-cell contents efficiently [27]. In cancer, chemotherapeutic drugs retrieve the balance between apoptotic and survival signals by specifically targeting cells with a high division rate. PTX is known to halt the mitotic division leading to cell cycle arrest and apoptosis [21]; in our current study, we evaluated the effect of SFN on PTX-induced cell cycle arrest and apoptosis in the PC-3 prostate cancer cell line. Our data confirmed that SFN significantly improved PTX-induced activation of caspase-3 and increased the number of accumulated cells in the S-growth phase (S-growth phase arrest). Such changes were accompanied by the appearance of apoptotic bodies and micro-nuclei in the treated cells. Interestingly, PTX + SFN combined treatment did not increase the numbers of necrotic cells comparable to PTX or SFN individual treatments. These data indicate that SFN augmented the potency of PTX as an anticancer agent and at the same time did not increase necrosis, which is one of PTX's side effects.

One of the strategies that a cancer cell adopts to evade apoptosis is to upregulate the expression of survival signaling proteins, such as Bcl_2, which showed higher levels in prostate cancer [28, 29]. The elevated Bcl_2 mRNA and protein levels were specifically reported in the prostate cancer cell line (LNCaP) [30]. Higher levels of Bcl_2 inhibit caspases activities and result in resistance to apoptosis by preventing the release of cytochrome *c* from the mitochondria [31]. Additionally, other researchers reported that Bcl_2 binds to the apoptosis-activating factor (APAF-1) [32]; therefore, we proposed that lowering Bcl_2 levels may sensitize transformed cells to anticancer drugs, such as PTX. The data presented here confirmed that PTX in combination with SFN additively reduced the level of Bcl_2 protein compared with PTX or SFN alone in both prostate cancer cell models (PC-3 and LNCaP). This result is consistent with previously published reports, where inhibiting Bcl_2 using nonpeptide small molecules inhibitors improved the therapeutic outcomes for targeting prostate cancer cells [33, 34]. Furthermore, the ratio of Bax (pro-apoptotic Bcl_2 family member): Bcl_2 protein levels are crucial for cell survival [35], where increasing Bax levels overcome the threshold that Bcl_2 can neutralize, Bax, translocation to the mitochondria, leading to the release of cytochrome *c* and trigger apoptosis [36]. So that we investigated the levels of Bax protein following different treatments and calculated Bax: Bcl_2 ratio. Our data indicated that combination therapy of PTX and SFN significantly increased Bax protein expression and Bax: Bcl_2 ratio compared to PTX or SFN individual treatments in both PC-3 and LNCaP cells.

Conclusion

Although PTX therapy had been a big success in cancer treatment, its clinical efficacy was limited to its increasing side effects and acquired resistance. The SFN may enhance the efficacy of PTX in targeting prostate cancer cell lines (PC-3) and (LNCaP). Resistance to PTX and anti-cancer doses of PTX was reduced when PTX and SFN

metabolites were combined, therefore increasing the need for further investigations in which we could utilize *in-vivo* studies in pursuit of prostate cancer management.

Abbreviations

SFN: sulforaphane; PTX: Paclitaxel/ or Taxol; BPH: Benign prostatic hypertrophy; Nrf2: Nuclear factor-erythroid-2-related factor 2; PPAR-γ: Peroxisome proliferator-activated γ; PSA: Prostate-specific antigen; HDAC3: Upregulated histone deacetylase protein; DMSO: Dimethyl sulfoxide; MTT: Thiazolyl blue tetrazolium bromide; RIPA: Radioimmunoprecipitation assay buffer; SDS: Sodium dodecyl sulfate; anti-GAPDH: anti-glyceraldehyde-3-phosphate dehydrogenase; DAPI: 4',6-diamidino-2-phenylindole; PBS: Phosphate-buffered saline; PI: Propidium Iodide; APAF: Apoptosis-activating factor.

Declarations

Acknowledgments

All thanks and appreciation to the Faculty of Science, Sohag University to provide us with the necessary chemicals and equipment for the experimental part of this study. Special thanks to Dr. Ali Fahmy (Vacsera Vaccination Centers), Prof. of Molecular Toxicology, for providing the PC-3 cell lines, cell cycle analysis (Flow Cytometry Laboratory), and MTT assays.

Author Contributions

T.N. Habib, M.O. Altonsy, M.S. Salama, Supervision, study design, data analysis, and discussion.

T.N. Habib, M.A. Hosny, Methodology, data collection, writing-review & editing.

S.A. Ghanem, Data analysis, Methodology.

All authors reviewed the manuscript.

Conflicts of Interest

Conflict of interest relevant to this article was not reported.

Funding

This study is issued from an M.Sc. The thesis of Mai Hosny was financially funded by the Zoology Department, Faculty of Science, Sohag University.

Availability of data and materials

The datasets used and/or analyzed during the current study are available from the corresponding author on reasonable request.

Consent for publication

Not applicable.

Competing interests

The authors declare that they have no competing interests.

References

1. Mattiuzzi C, Lippi G. Current Cancer Epidemiology. J. Epidemiol. Glob. Health. 2019 Dec;9(4):217–222. doi: 10.2991/jegh.k.191008.001. PMID: 31854162; PMCID: PMC7310786.
2. Singh O, Bolla SR. Anatomy, Abdomen and Pelvis, Prostate. 2021 Jul 26. In: StatPearls [Internet]. Treasure Island (FL): StatPearls Publishing; 2022 Jan– PMID: 31082031.
3. Kraemer PC, Borre M. Aflastning af tumorbetinget obstruerede øvre urinveje ved prostatacancer [Relief of upper urinary tract obstruction in patients with cancer of the prostate]. Ugeskr Laeger. 2009 Mar 9;171(11):873–6. Danish. PMID: 19278608.
4. Gann PH. Risk factors for prostate cancer. Rev Urol. 2002;4 Suppl 5(Suppl 5):S3-S10. PMID: 16986064; PMCID: PMC1476014.
5. Niclis C, Díaz Mdel P, Eynard AR, Román MD, La Vecchia C. Dietary habits and prostate cancer prevention: a review of observational studies by focusing on South America. Nutr Cancer. 2012;64(1):23–33. doi: 10.1080/01635581.2012.630163. Epub 2011 Dec 2. PMID: 22136636.
6. Hu FB. Dietary pattern analysis: a new direction in nutritional epidemiology. Curr Opin Lipidol. 2002 Feb;13(1):3–9. doi: 10.1097/00041433-200202000-00002. PMID: 11790957.
7. Niclis C, Román MD, Osella AR, Eynard AR, Díaz Mdel P. Traditional Dietary Pattern Increases Risk of Prostate Cancer in Argentina: Results of a Multilevel Modeling and Bias Analysis from a Case-Control Study. J. Cancer Epidemiol. 2015;2015:179562. doi: 10.1155/ 2015/179562. Epub 2015 Nov 16. PMID: 26649040; PMCID: PMC4663343.
8. Shinkai Y, Sumi D, Fukami I, Ishii T, Kumagai Y. Sulforaphane, an activator of Nrf2, suppresses cellular accumulation of arsenic and its cytotoxicity in primary mouse hepatocytes. FEBS Lett. 2006 Mar 20;580(7):1771-4. doi: 10.1016/j.febslet.2006.02.031. Epub 2006 Feb 24. PMID: 16516206.
9. Mahn A, Castillo A. Potential of Sulforaphane as a Natural Immune System Enhancer: A Review. Molecules. 2021 Feb 1;26(3):752. doi: 10.3390/molecules26030752. PMID: 33535560; PMCID: PMC7867070.
10. Moi P, Chan K, Asunis I, Cao A, Kan YW. Isolation of NF-E2-related factor 2 (Nrf2), a NF-E2-like basic leucine zipper transcriptional activator that binds to the tandem NF-E2/AP1 repeat of the beta-globin locus control region. Proc Natl Acad Sci U S A. 1994 Oct 11;91(21):9926-30. doi: 10.1073/pnas.91.21.9926. PMID: 7937919; PMCID: PMC44930.
11. Zhang Y, Talalay P, Cho CG, Posner GH. A major inducer of anticarcinogenic protective enzymes from broccoli: isolation and elucidation of structure. Proc Natl Acad Sci U S A. 1992 Mar 15;89(6):2399 – 403. doi: 10.1073/pnas.89.6.2399. PMID: 1549603; PMCID: PMC48665.
12. Prochaska HJ, Santamaria AB, Talalay P. Rapid detection of inducers of enzymes that protect against carcinogens. Proc. Natl. Acad. Sci. USA. 1992 Mar. 15;89(6):2394-8. doi: 10.1073/ pnas.89.6.2394. PMID: 1549602; PMCID: PMC48664.
13. Hayes JD, McMahon M. NRF2 and KEAP1 mutations: permanent activation of an adaptive response in cancer. Trends Biochem. Sci. 2009 Apr;34(4):176–88. doi: 10.1016/j.tibs.2008. 12.008. Epub 2009 Mar 25. PMID: 19321346.

14. Surh YJ, Kundu JK, Na HK. Nrf2 as a master redox switch in turning on the cellular signaling involved in the induction of cytoprotective genes by some chemopreventive phytochemicals. Planta Med. 2008 Oct;74(13):1526–39. doi: 10.1055/s-0028-1088302. Epub 2008 Oct 20. PMID: 18937164.
15. Kwak MK, Wakabayashi N, Kensler TW. Chemoprevention through the Keap1-Nrf2 signaling pathway by phase 2 enzyme inducers. Mutat. Res. 2004 Nov. 2;555(1–2):133 – 48. doi: 10.1016/j.mrfmmm.2004.06.041. PMID: 15476857.
16. Brooks JD, Paton VG, Vidanes G. Potent induction of phase 2 enzymes in human prostate cells by sulforaphane. Cancer Epidemiol. Biomarkers Prev. 2001 Sep;10(9):949–54. PMID: 11535546.
17. Singh SV, Srivastava SK, Choi S, Lew KL, Antosiewicz J, Xiao D, Zeng Y, Watkins SC, Johnson CS, Trump DL, Lee YJ, Xiao H, Herman-Antosiewicz A. Sulforaphane-induced cell death in human prostate cancer cells is initiated by reactive oxygen species. J Biol Chem. 2005 May 20;280(20):19911-24. doi: 10.1074/jbc.M412443200. Epub 2005 Mar 11. PMID: 15764812.
18. Cipolla BG, Mandron E, Lefort JM, Coadou Y, Della Negra E, Corbel L, Le Scodan R, Azzouzi AR, Mottet N. Effect of Sulforaphane in Men with Biochemical Recurrence after Radical Prostatectomy. Cancer Prev Res (Phila). 2015 Aug;8(8):712–9. doi: 10.1158/1940-6207.CAPR-14-0459. Epub 2015 May 12. PMID: 25968598.
19. Beaver LM, LÓ§hr CV, Clarke JD, Glasser ST, Watson GW, Wong CP, Zhang Z, Williams DE, Dashwood RH, Shannon J, Thuillier P, Ho E. Broccoli Sprouts Delay Prostate Cancer Formation and Decrease Prostate Cancer Severity with a Concurrent Decrease in HDAC3 Protein Expression in Transgenic Adenocarcinoma of the Mouse Prostate (TRAMP) Mice. Curr Dev Nutr. 2017 Dec 26;2(3):nzy002. doi: 10.1093/cdn/nzy002. PMID: 30019025; PMCID: PMC6041877.
20. Bayat Mokhtari R, Homayouni TS, Baluch N, Morgatskaya E, Kumar S, Das B, Yeger H. Combination therapy in combating cancer. Oncotarget. 2017 Jun 6;8(23):38022–38043. doi: 10.18632/oncotarget.16723. PMID: 28410237; PMCID: PMC5514969.
21. Weaver BA. How Taxol/paclitaxel kills cancer cells. Mol Biol Cell. 2014 Sep 15;25(18):2677-81. doi: 10.1091/mbc.E14-04-0916. PMID: 25213191; PMCID: PMC4161504.
22. Rationalizing combination therapies. Nat Med. 2017 Oct 6;23(10):1113. doi 10.1038/nm.4426. PMID: 28985211.
23. Rivera E, Gomez H. Chemotherapy resistance in metastatic breast cancer: the evolving role of ixabepilone. Breast Cancer Res. 2010;12 Suppl 2(Suppl 2):S2. doi: 10.1186/bcr2573. Epub 2010 Oct 22. PMID: 21050423; PMCID: PMC2972556.
24. Gjyrezi A, Xie F, Voznesensky O, Khanna P, Calagua C, Bai Y, Kung J, Wu J, Corey E, Montgomery B, Mace S, Gianolio DA, Bubley GJ, Balk SP, Giannakakou P, Bhatt RS. Taxane resistance in prostate cancer is mediated by decreased drug-target engagement. J Clin Invest. 2020 Jun 1;130(6):3287–3298. doi: 10.1172/JCI132184. PMID: 32478682; PMCID: PMC7259995.
25. Levin L, Hryniuk WM. Dose intensity analysis of chemotherapy regimens in ovarian carcinoma. J Clin Oncol. 1987 May;5(5):756 – 67. doi: 10.1200/JCO.1987.5.5.756. PMID: 3572465.
26. Elmore S. Apoptosis: a review of programmed cell death. Toxicol Pathol. 2007 Jun;35(4):495–516. doi: 10.1080/01926230701320337. PMID: 17562483; PMCID: PMC2117903.
27. Nanji AA, Hiller-Sturmhöfel S. Apoptosis and necrosis: two types of cell death in alcoholic liver disease. Alcohol Health Res World. 1997;21(4):325–30. PMID: 15706744; PMCID: PMC6827678.

28. Karnak D, Xu L. Chemosensitization of prostate cancer by modulating Bcl-2 family proteins. Curr Drug Targets. 2010 Jun;11(6):699–707. doi: 10.2174/138945010791170888. PMID: 20298153; PMCID: PMC2998062.
29. Chaudhary KS, Abel PD, Lalani EN. Role of the Bcl-2 gene family in prostate cancer progression and its implications for therapeutic intervention. Environ Health Perspect. 1999 Feb;107 Suppl 1(Suppl 1):49–57. doi: 10.1289/ehp.99107s149. PMID: 10229706; PMCID: PMC1566368.
30. Lin Y, Fukuchi J, Hiipakka RA, Kokontis JM, Xiang J. Up-regulation of Bcl-2 is required for the progression of prostate cancer cells from an androgen-dependent to an androgen-independent growth stage. Cell Res. 2007 Jun;17(6):531-6. doi: 10.1038/cr.2007.12. PMID: 17404601.
31. Yang J, Liu X, Bhalla K, Kim CN, Ibrado AM, Cai J, Peng TI, Jones DP, Wang X. Prevention of apoptosis by Bcl-2: release of cytochrome c from mitochondria blocked. Science. 1997 Feb 21;275(5303):1129-32. doi: 10.1126/science.275.5303.1129. PMID: 9027314.
32. Haraguchi M, Torii S, Matsuzawa Si, Xie Z, Kitada S, Krajewski S, Yoshida H, Mak TW, Reed JC. Apoptotic protease activating factor 1 (Apaf-1)-independent cell death suppression by Bcl-2. J Exp Med. 2000 May 15;191(10):1709–20. doi: 10.1084/jem.191.10.1709. PMID: 10811864; PMCID: PMC2193150.
33. Suleiman MR, Wang H, Huang D, Wang H, Joseph J, Huang T, Zhang F, Wang J, Cheng M. Discovery of small molecule inhibitors through pharmacophore modeling, molecular docking, molecular dynamics simulation and experimental validation against myeloid cell leukemia-1 (Mcl-1). J. Biomol. Struct. Dyn. 2021 Apr;39(7):2512–2525. doi: 10.1080/07391102. 2020.1749132. Epub 2020 Apr 20. PMID: 32228162.
34. Wang S, Yang D, Lippman ME. Targeting Bcl-2 and Bcl-XL with nonpeptidic small-molecule antagonists. Semin Oncol. 2003 Oct;30(5 Suppl 16):133–42. doi: 10.1053/j.seminoncol.2003. 08.015. PMID: 14613034.
35. Korsmeyer SJ. Bcl-2: an antidote to programmed cell death. Cancer Surv. 1992;15:105–18. PMID: 1451107.
36. Edlich F, Banerjee S, Suzuki M, Cleland MM, Arnoult D, Wang C, Neutzner A, Tjandra N, Youle RJ. Bcl-x(L) retrotranslocates Bax from the mitochondria into the cytosol. Cell. 2011 Apr 1;145(1):104 – 16. doi: 10.1016/j.cell.2011.02.034. PMID: 21458670; PMCID: PMC3070914.

Figures

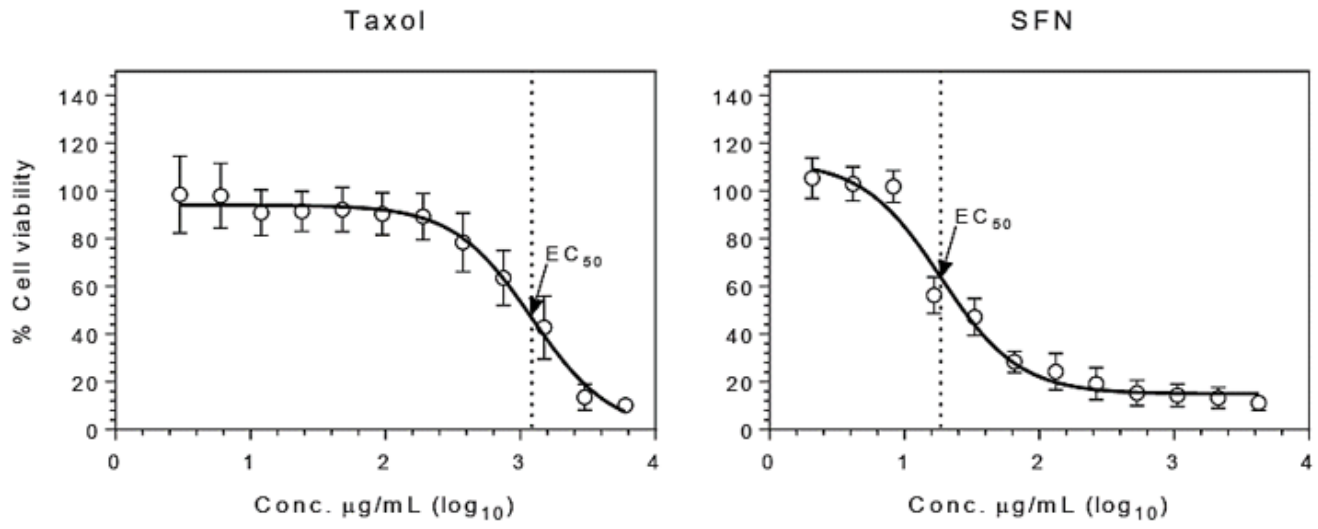

Figure 1

Prostate cancer PC-3 Cell viability dose-response curves and (EC_{50}) of PTX (A) and SFN (B). PC-3 cells were grown in 48-well plates at a density of 35,000 cells/well and incubated at 37°C and 5% CO_2 atmosphere for 24 h. Cells were treated with different concentrations of PTX or SFN. Cell viability tests were performed 24 h post-treatment using an MTT assay to measure cellular metabolic activity as an indicator of cell viability as described in the methods section. Collected data analysis and EC_{50} calculations for each drug were carried out using Graph-Pad Prism software. Data *n* = 4, expressed as mean values with ±SD error bars.

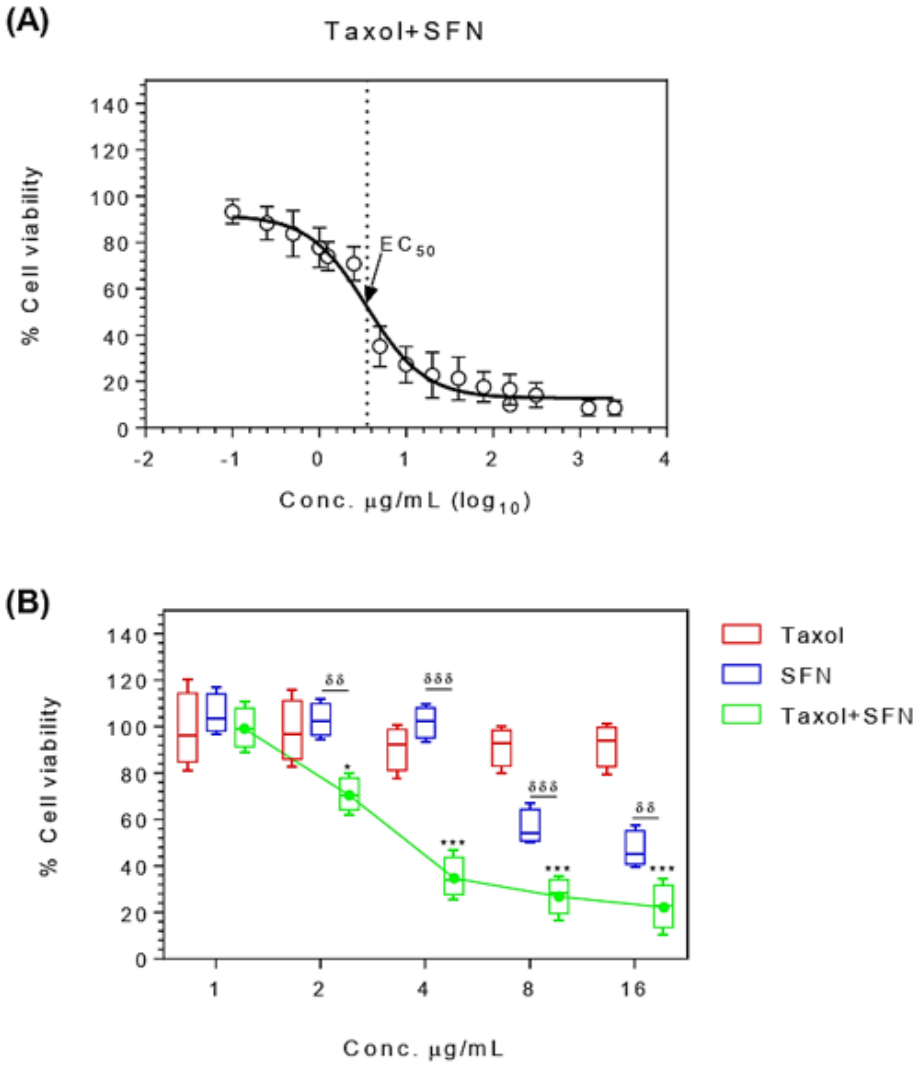

Figure 2

The SFN synergized PTX's effect on reducing cell viability in PC-3 cells. (A) To determine the EC_{50} of the combined treatment, PTX and SFN were diluted in culturing medium at equal concentrations ranging from 100 ng/ml to 2500 µg/ml and used to treat PC-3 cells. MTT cell viability assay was conducted 24 h after treatment. **(B)** In a comparison between cell viability values in response to individual treatment (PTX or SFN) and combined treatment (PTX+SFN), cell viability values of non-stimulated cells were considered as 100% for each administered

concentration. Data n = 5, was analyzed with the GraphPad Prism 6 software and presents as a mean with ±SD error bars in **(A)**, or box-and-whisker plots in **(B)**. Student's t-test (for two groups comparison) was used to determine the significant difference between PTX and PTX+SFN, *$p \leq 0.05$, **$p \leq 0.01$, ***$p \leq 0.001$, or between SFN and PTX+SFN, *$p \leq 0.05$, **$p \leq 0.01$.

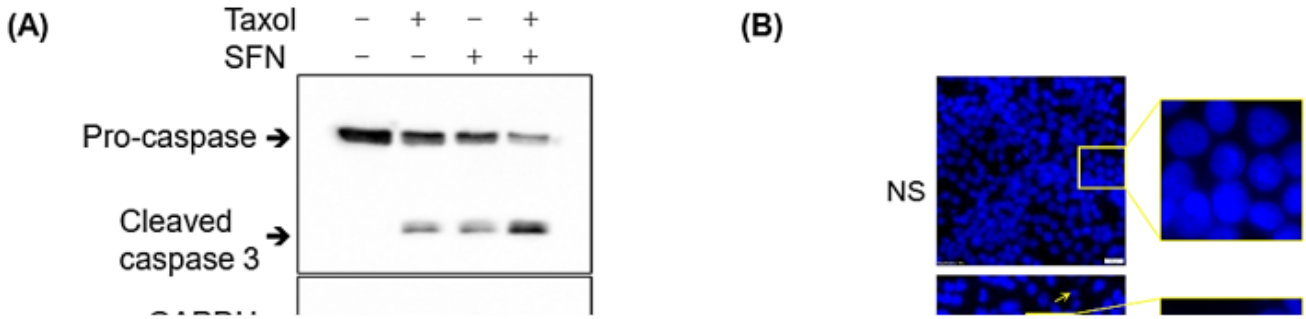

Figure 3

The SFN additively enhanced PTX-induced apoptosis in PC-3 cells. (A) Western blot and densitometric analysis of caspase-3 protein bands separated by SDS-PAGE from PC-3 cells' lysate pre-treated with PTX (1.2 mg/ml), SFN (18.7 µg/ml), or PTX+SFN combination for 24 h. Blot graph (upper) showed cleaved caspase-3 bands in PTX, SFN, and PTX+SFN treated cells, but not in non-stimulated cells. Densitometric quantification (bottom) demonstrated significantly higher bands-intensity of cleaved caspase-3 in PTX+SFN than PTX or SFN individual treatments. This was accompanied by a reduction in pro-caspase-3 bands (the inactive form of caspase-3 protein). **(B)** Fluorescent micrographs of PC-3 cells stained with DAPI show nuclear fragmentation (boxes) and micro-nuclei formations (arrows) in PC-3 cells treated with the aforementioned concentrations of PTX, SFN, or PTX+SFN for 24 h. Data n = 5, and pro-and active caspase-3 bands intensities were presented as box-and-whiskers plots. Student's t-test (for

two groups comparison) was used to determine the significant difference between PTX or SFN individual treatments and PTX+SFN combined treatments, ***$p \leq 0.001$.

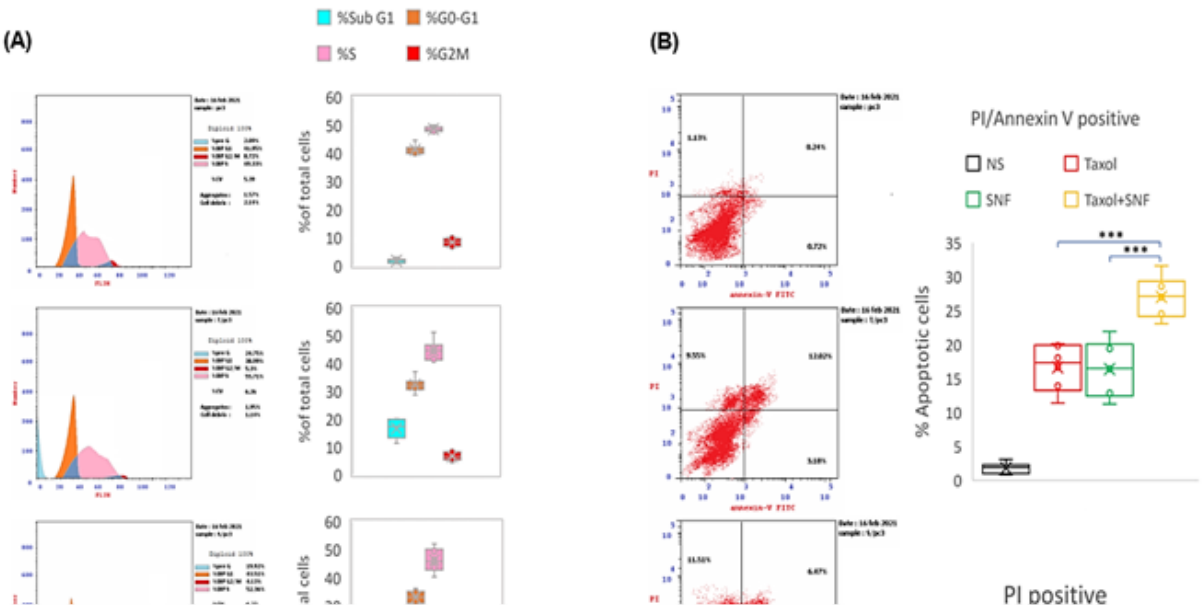

Figure 4

SFN enhanced PTX-induced cell-cycle arrest and apoptosis without affecting the number of necrotic PC-3 cells. (A) Flow cytometry histogram and box-and-whiskers plots of Cell-cycle analysis of PC-3 cells stained with PI show the effect of PTX, SFN, or PTX+SFN treatments on cell-cycle growth phases and the numbers of apoptotic cells (sub-G1 population). **(B)** scatter dots and box-and-whiskers plots of PC-3 cells double-stained with PI and annexin V to differentiate between apoptotic and necrotic effects of PTX, SFN, or PTX+SFN treatments. Data $n = 5$, significant differences were determined using Student's t-test (for two groups comparison), ***$p \leq 0.001$.

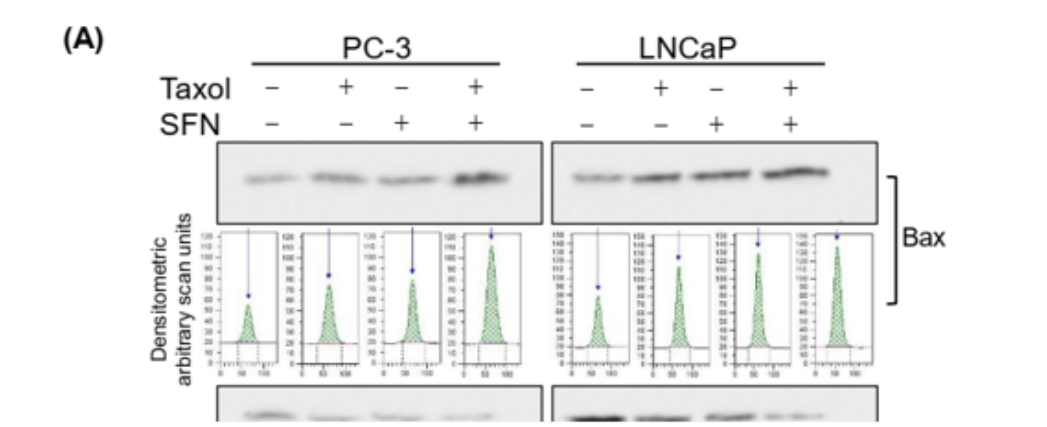

Figure 5

PTX and/or SFN modulate the expression of apoptotic signaling proteins in PC-3 and LNCaP cells. (A) Western blots (top) and densitometric analysis histograms (bottom) show the effect of PTX, SFN, or PTX+SFN treatments on the expression of Bax and Bcl_2 proteins in PC-3 and LNCaP cells. GAPDH, the housekeeping protein, was used as a loading control marker. **(B)** Box-and-whiskers plot demonstrates the effect of PTX, SFN, or PTX+SFN treatments on Bax: Bcl_2 ratios in PC-3 and LNCaP cells. Data $n = 5$. The significant differences between non-stimulated cells and PTX, SFN, or PTX+SFN-treated cells, $^{**}p \leq 0.01$, $^{***}p \leq 0.001$, or between PTX and PTX+SFN-treated cells $^{***}p \leq 0.001$, were determined using Student's t-test (for two groups comparison).

Supplementary Files

This is a list of supplementary files associated with this preprint. Click to download.

- RawDataSulforaphane.xlsx